



Rotation Periods of Asteroids Determined With Bootstrap Convex Inversion From ATLAS Photometry

Josef Ďurech^{1*}, Michael Vávra¹, Radim Vančo¹ and Nicolas Erasmus²

¹Astronomical Institute, Faculty of Mathematics and Physics, Charles University, Prague, Czech Republic, ²South African Astronomical Observatory, Cape Town, South Africa

OPEN ACCESS

Edited by:

Daniel Hestroffer,
Université de Sciences Lettres de
Paris, France

Reviewed by:

Alan Harris,
NASA Jet Propulsion Laboratory
(JPL), United States
Jianguo Yan,
Wuhan University, China

*Correspondence:

Josef Ďurech
durech@sirrah.troja.mff.cuni.cz

Specialty section:

This article was submitted to
Astrostatistics,
a section of the journal
Frontiers in Astronomy and Space
Sciences

Received: 05 November 2021

Accepted: 17 January 2022

Published: 22 February 2022

Citation:

Ďurech J, Vávra M, Vančo R and
Erasmus N (2022) Rotation Periods of
Asteroids Determined With Bootstrap
Convex Inversion From
ATLAS Photometry.
Front. Astron. Space Sci. 9:809771.
doi: 10.3389/fspas.2022.809771

The rotation period is one of the fundamental physical characteristics of asteroids. It can be determined from photometric measurements by standard methods of time-series period analysis or by creating a physical model of an asteroid with the rotation period being one of the fitted parameters. We used the latter approach to determine the sidereal rotation period for more than 5000 asteroids, out of which about 1600 are those for which their period was not known. We processed photometric measurements of about 100,000 asteroids from the ATLAS survey with the light curve inversion technique in the Asteroids@home project to search for the best-fit rotation period. This was repeated 25 times with randomly resampled—bootstrapped—data. For thousands of asteroids, their best-fit period was the same for most of the bootstrapped data sets; thus, their rotation period was determined with a high degree of reliability.

Keywords: asteroids, photometry, surveys, light curves, bootstrap

1 INTRODUCTION

Asteroid photometry is a simple yet powerful tool to reveal some basic physical properties of observed objects. Time-resolved photometry—a light curve—provides a direct measurement of the rotation period. The vast majority of asteroid rotation periods (currently around 30,000 in the Asteroid Lightcurve Database, LCDB, of Warner et al., 2009)¹ have been determined from light curve analysis.

When an asteroid is observed over a longer time interval (years), its light curves change as the aspect and the solar phase angle change. If the coverage of geometries is sufficient (which usually requires several apparitions for a main-belt asteroid), the evolving shape of the light curves uniquely defines the direction of the rotation axis and the convex shape of the asteroid, together with the sidereal rotation period (Kaasalainen and Ďurech, 2020). The process of reconstruction of asteroid shape and spin is called light curve inversion, and it can be done almost routinely if there is a sufficient amount of observations (Kaasalainen et al., 2001, 2002).

Apart from classical light curves that are true “curves” showing how the brightness evolves with time, there are also photometric observations that are sparse with respect to the rotation period. Thus, instead of a curve, we have individual sparse-in-time brightness measurements. This data type are typically produced by sky surveys and they can be used the same way as light curves for the shape and spin reconstruction of asteroids (Kaasalainen, 2004).

¹<https://minplanobs.org/MPInfo/>

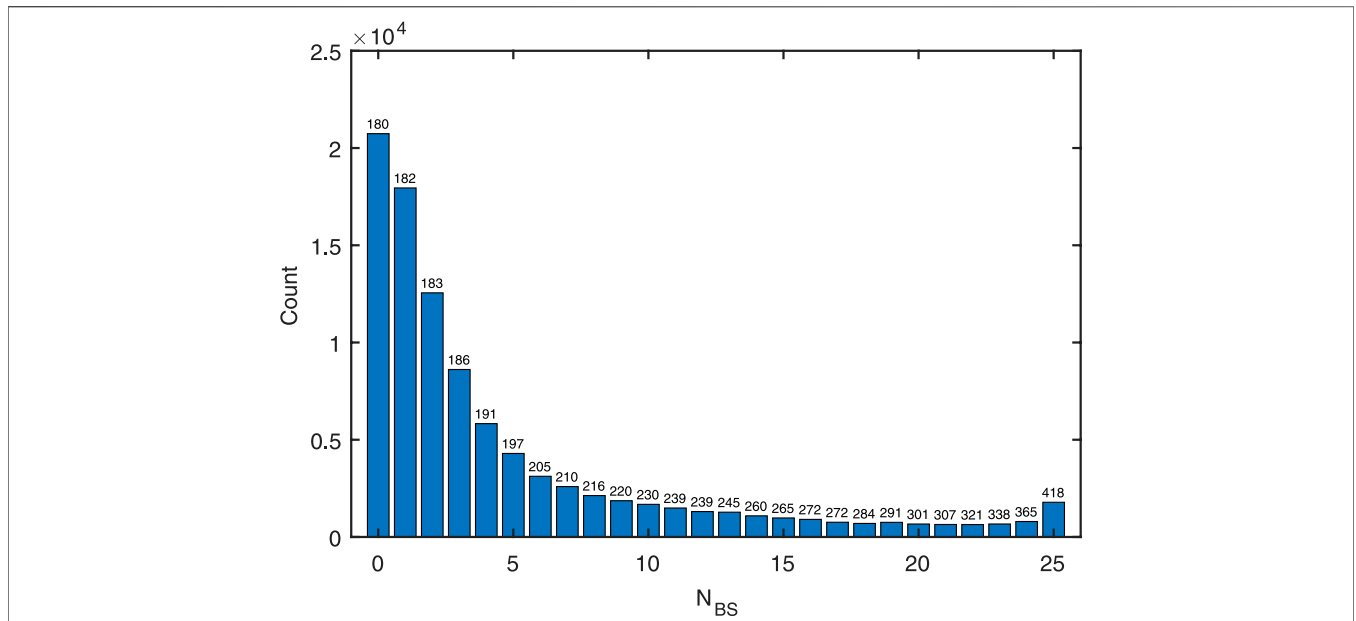


FIGURE 1 | Histogram showing the number of asteroids with a given N_{BS} —the number of cases in which the BS period was the same as the original one. The number above each histogram bar indicates the mean number of data points for asteroids in that sample.

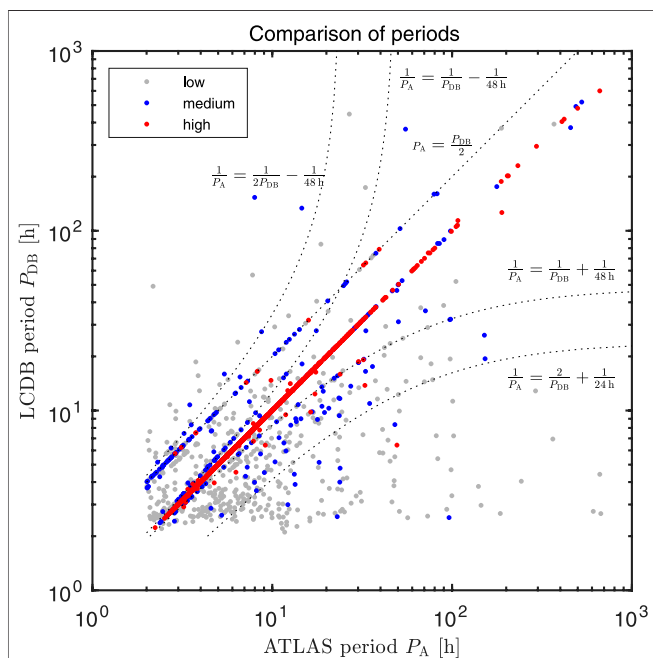


FIGURE 2 | Comparison of periods P_A derived from ATLAS data with the LCDB periods P_{DB} for three different groups: low-reliability ($1 \leq N_{BS} \leq 6$), medium-reliability ($10 \leq N_{BS} \leq 15$), and high-reliability ($10 \leq N_{BS} \leq 25$). The dotted curves indicate 24 or 48 h aliases and half-period alias that are common for less reliable periods.

With the light curve inversion, the shape and spin of an asteroid are found by fitting a model (described by the rotation period P , the direction of the spin axis in ecliptic

coordinates (λ, β) , and parameters of a convex shape) to data. The best model is found by scanning the period/pole parameter space with the standard χ^2 measure used to define the best agreement between the model and the data. Hundreds of models have been derived from dense photometry (Wang et al., 2015; Warner et al., 2017; Husárik, 2018; Marciniak et al., 2018; Franco and Pilcher, 2020, for example) and thousands from sparse photometry (Ďurech et al., 2009; Hanuš et al., 2013; Ďurech et al., 2016; Ďurech and Hanuš, 2018; Ďurech et al., 2020, for example). Sparse photometry is available from large sky-surveys (Pan-STARRS, ATLAS, Catalina, Gaia, ZTF, etc.) essentially for all asteroids. Because the photometric accuracy and the number of data points are usually not sufficient to derive a reliable model, the success rate of inversion of sparse data is low. However, as we show in this paper even when sparse data are not abundant enough to derive a reliable full spin/shape model, the rotation period can be derived uniquely.

This work aims to derive sidereal rotation periods of asteroids that have photometric data from the ATLAS survey. In our previous work (Ďurech et al., 2020), we used the same data to derive full shape/spin models.

2 ATLAS PHOTOMETRY

In this work, we used the same data set as Ďurech et al. (2020). The data come from the Asteroid Terrestrial-impact Last Alert System (ATLAS) telescopes located in Hawaii (Tonry et al., 2018b,a; Smith et al., 2020; Heinze et al., 2018) and consist of photometric measurements collected from June 2015 to October 2018 in orange (*o*, 560–820 nm) and cyan (*c*, 420–650 nm) filters.

TABLE 1 | For nine groups of asteroids with different N_{BS} , the table lists the number N_A of asteroids with a given N_{BS} , the number N_{US} of those that have $U = 3$ period record in the LCDB, the number N_{same} of asteroids with the P_A and P_{DB} being the same ($\pm 5\%$), the probability $p_{same} = N_{same}/N_{US}$, the number of wrong ATLAS periods N_A^{wrong} (Table 2), the number of wrong LCDB periods N_{DB}^{wrong} (Table 2), and the probability $p_A^{correct}$ that P_A is correctly determined.

N_{BS}	N_A	N_{US}	N_{same}	p_{same} [%]	N_A^{wrong}	N_{DB}^{wrong}	p_{DB}^{wrong}	$p_A^{correct}$ [%]
25	1784	904	885	97.9	4	14	1.6	99.5
24	795	231	224	97.0	2	4	1.8	98.6
23	667	165	159	96.4	3	2	1.3	97.9
22	639	114	109	95.6	4	1	0.9	97.2
21	642	114	105	92.1				93.6
20	666	99	91	91.9				93.4
19	752	106	90	84.9				86.3
18	696	72	56	77.8				79.0
17	757	74	60	81.1				82.4

The original data set consisted of photometry of about 180,000 asteroids. However, we selected only asteroids with at least 100 observations, which reduced the total number of objects to about 100,000.

We processed this data set at Asteroids@home project (Ďurech et al., 2015)—the best-fit sidereal rotation period was searched for at an interval of 2–1,000 h, and ten initial spin axis directions were tried for each trial period. The spin and shape parameters then converged to a local minimum in χ^2 . The global minimum in χ^2 then defined the best-fit sidereal rotation period P_A . This part of the work was, in fact, ready because we used the periodograms computed already by Ďurech et al. (2020). In our previous work (Ďurech et al., 2020), we selected the global minimum in χ^2 , tested its significance with respect to other global minima, checked the reliability of the shape model using the same processing pipeline as Ďurech et al. (2018), and reported the shape models with their rotation poles and periods. In our new approach, we concentrated only on rotation periods. We used a bootstrap (BS) method to resample the observations randomly and determine the period and its uncertainty via a Monte Carlo approach. We repeated the period scan for each BS realization, generated a new periodogram, and tested the robustness of the original best-fit period P_A .

3 BOOTSTRAP

For each asteroid, we created 25 bootstrapped samples of the original data set in both filters independently (we randomly selected the same number of measurements) and repeated the period search, i.e., we computed other 25 periodograms at Asteroids@home. From each periodogram, we selected the best-fit period $P_{BS}^{(i)}$ defined as having the minimum χ^2 value. This way, we obtained for each asteroid (95 789 in total) 25 best periods $P_{BS}^{(i)}$, $i = 1, \dots, 25$, from bootstrapped data. We decided to compute 25 BS samples as a compromise between the robustness of our analysis and the computational time spent on Asteroids@home.

The motivation for this approach was our expectation that if the best period is always the same for all BS samples, it is likely to be the actual rotation period. On the other hand, if the original period P_A is not found in resampled BS data, it is likely just a random value not related to the real rotation period. Figure 1 shows the distribution of N_{BS} , which is the number of cases when the best BS period $P_{BS}^{(i)}$ was the same as the original period P_A . By “the same” we mean that their relative difference was not larger than 1%. In other words, for each asteroid, we define

$$N_{BS} = \sum_{i=1}^{25} \xi_i, \text{ where } \xi_i = 1 \text{ if } \frac{|P_A - P_{BS}^{(i)}|}{P_A} \leq 0.01, \text{ and } \xi_i = 0 \text{ otherwise.}$$

If every BS sample gives the same best-fit period, then $N_{BS} = 25$. If no $P_{BS}^{(i)}$ agrees with the original P_A , then $N_{BS} = 0$. As we can see in Figure 1, for about 20,000 asteroids, the best period in each BS sample is just a random value that is, not related to the original period—the number of agreements N_{BS} is zero. The majority (about 70,000) asteroids have no more than five cases in which P_{BS} agrees with P_A , their $N_{BS} \leq 5$. As expected, the number of asteroids with some value of N_{BS} decreases with increasing N_{BS} until the maximum $N_{BS} = 25$. The number of asteroids for which all 25 BS samples give the same period as the original data is ~1800. The number of observations plays a crucial role in the robustness of period determination—the mean number of data points for asteroids in each histogram bar is shown in Figure 1; it increases with increasing N_{BS} . The minimum number of observations was 100. Asteroids with uncertain periods ($N_{BS} \leq 5$) have, on average, less than 200 observations; those with almost certain period determination ($N_{BS} \geq 20$) have more than 300.

In Figure 2, we show a comparison between periods P_A determined from the original ATLAS data and periods P_{DB} taken from the LCDB of Warner et al. (2009) with the uncertainty tag $U = 3$ (release from June 2021, 3830 asteroids with $U = 3$). The uncertainty tag evaluates the reliability of the period and $U = 3$, the highest value, means that the period is unambiguous and uniquely determined. Asteroids with high N_{BS} (red points, $20 \leq N_{BS} \leq 25$) lie primarily on the diagonal, which means that the periods P_{LCDB} and P_A are the same. For medium-reliability period determinations (blue points, $10 \leq N_{BS} \leq 15$), many P_A values do not agree with the LCDB period, and often there is an alias of 24 or 48 h; or P_A is half of P_{DB} . For the low-reliability group (grey points, $1 \leq N_{BS} \leq 6$), there is no apparent relation between the two periods— P_A periods are just arbitrary values not reliable at all.

3.1 Reliability of Period Determination

Out of the total sample of ~100,000 asteroids, 1784 have $N_{BS} = 25$, i.e., all BS realizations lead to the same best-fit period, so these are those asteroids with the most reliable period determination. Out of them, 904 also have a period compiled in the LCDB with $U = 3$, which enables us to compare our ATLAS periods with independent values. We assume that P_{DB} and P_A agree if their relative difference is less than 5%. For 885 cases, the ATLAS period agrees with P_{DB} . However, 19 asteroids have different periods; they are listed in Tables 1, 2. We checked the LCDB

TABLE 2 | List of asteroids with $N_{BS} \geq 22$ for which the period P_A that we obtained from ATLAS data disagrees with the period P_{DB} in the LCDB. The formal uncertainty of P_A is σ_{BS} . By “✓,” we mark our decision if either ATLAS period (A) or LCDB period (DB) is correctly determined. Behrend’s web is a database of asteroid light curve observations and rotation periods available at <https://obswww.unige.ch/behrend/page-cou.html>.

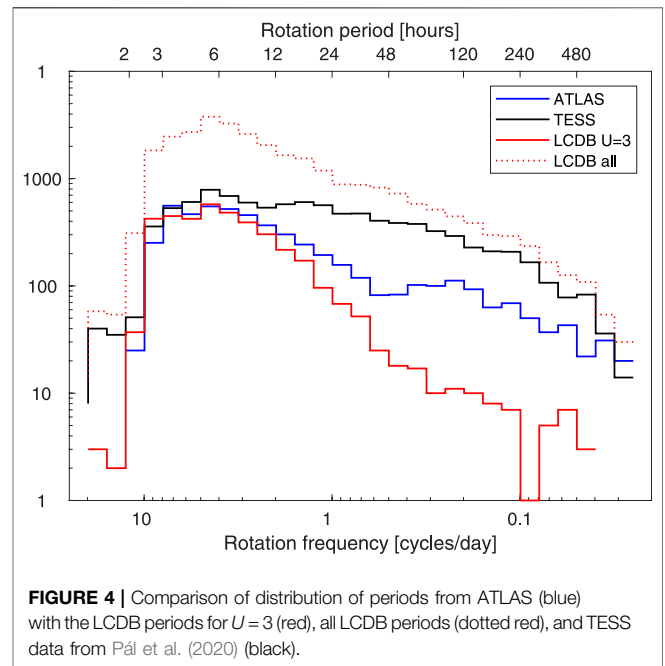
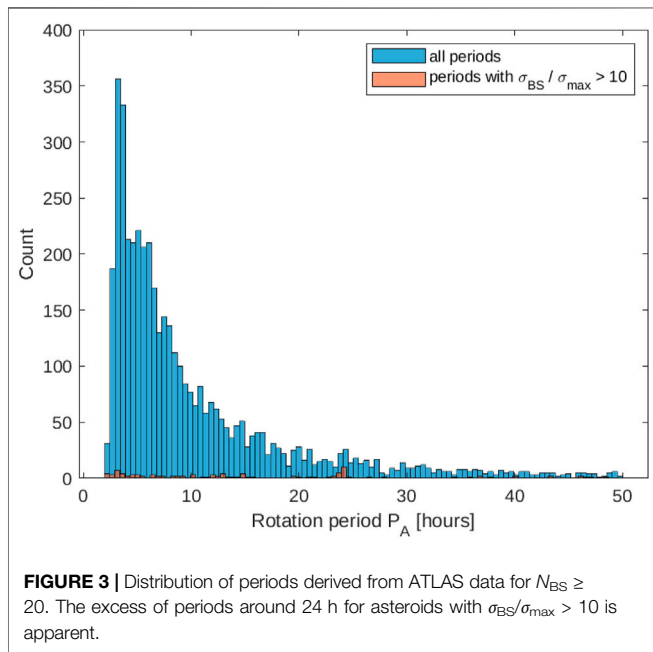
Asteroid	P_A (h)	σ_{BS} (h)	P_{DB} (h)	A	DB	Comment
$N_{BS} = 25$						
496 Gryphia	24.5152	0.0005	1072	✓	✓	The LCDB rotation period is outside the search interval. It is likely to be the correct period because the light curves of Pilcher et al. (2017) are flat with no apparent period of 24 h
526 Jena	11.8764	0.0004	9.474			Our P_A value is the same as the period determined by Ďurech et al. (2019) and is consistent also with light curves of Barucci et al. (1994), although they determined the period to 9.474 h
571 Dulcinea	189.12	0.03	126.3			According to Stephens (2011), this asteroid is a tumbler so there is no unique rotation period
818 Kapteynia	17.461	0.003	16.35	✓		Our period is likely to be correct because it is consistent with other sparse photometry (ASAS-SN, Hanuš et al., 2021). The LCDB period of 16.35 h (Stephens, 2002) might be just a result of incorrect folding of separate light curves
893 Leopoldina	12.5993	0.0003	14.115	✓		Ďurech et al. (2020) derived a full model with the same period from ATLAS data
1248 Jugurtha	12.19042	0.00003	12.91	✓		Our period is the same as an independent determination of Ďurech et al. (2016)
1332 Marconia	32.123	0.001	19.16	✓		Our period is the same as those derived by Devogèle et al. (2017), Ďurech et al. (2019)
1536 Pielinen	33.119	0.009	66.22		✓	The half period of 33 h was found using a convex model, the ellipsoidal model gives the correct period of 66 h. Also a full model derived from the same ATLAS data by Ďurech et al. (2020) has period of 66 h
1586 Thiele	3.296293	0.000009	3.086	✓		Our period is correct, the LCDB one is based on only two nights of Childers and Church (2007), likely incorrectly phased
1684 Iguassu	9.1434	0.0004	6.4156	✓		Our period is confirmed by independent results of Waszczak et al. (2015)
1786 Raahe	30.168	0.002	18.72	✓		Our period is correct—confirmed by independent sparse data and also Behrend’s database
3066 McFadden	32.7525	0.0005	13.798	✓		Pál et al. (2020) independently confirmed our period
3409 Abramov	8.50361	0.00004	7.791	✓		Erasmus et al. (2020) derived the same period from the same ATLAS data, other sparse photometry also confirms this period
3422 Reid	3.218274	0.000009	2.91	✓		Pál et al. (2020) found the same period
3507 Vilas	4.7550	0.00003	3.959	✓		The same period was found by Erasmus et al. (2020). Ďurech et al. (2020) derived a full model
5132 Maynard	3.6090	0.0001	3.902	✓		Independent confirmation of P_A by Pál et al. (2020)
6192 Javiergorosabel	39.317	0.002	78.85		✓	Our period is the same as Pál et al. (2020) but it corresponds to one-peak light curve, ellipsoidal model gives double period 78 h
9033 Kawane	2.88269	0.00002	5.7656	✓		The same as above, false half period
37 635 1993 UJ1	662.7	0.3	600	✓		The periods are similar although their difference is larger than 5%
$N_{BS} = 24$						
520 Franziska	8.25138	0.0003	16.507	✓	✓	Wrong half period
740 Cantabria	32.1410	0.006	64.453			Pál et al. (2020) and also Hanuš et al. (2021) report our P_A , Stephens et al. (2010) reports a value that is, twice larger
1227 Geranium	17.2683	0.004	12.363	?	?	Ďurech et al. (2020) derived the same period and a full model but the shape has an unrealistic triangular pole-on silhouette. Not clear which period is the correct one
1960 Guisan	7.84666	0.004	8.46	✓		Two low-quality light curves of Binzel (1987) probably incorrectly phased
2791 Paradise	16.3486	0.005	9.81	✓		Hanuš et al. (2016) reports period of 9.81 h (on a limited search interval) but Behrend’s web reports 16.361 h
4797 Ako	3.870091	0.00002	4.085	✓		Ďurech et al. (2020) derived a full model with the period close to that of Bennefeld et al. (2009)
11 087 Yamasakimakoto	6.279556	0.00004	4.5369	✓		Pál et al. (2020) confirm our period
$N_{BS} = 23$						
1539 Borrelly	23.8312	0.01	15.922	✓	✓	Behrend’s web and also Polakis (2020) confirm our period
2425 Shenzhen	9.838246	0.00002	14.715	✓		Confirmed by other sparse data and Ďurech et al. (2016)
2895 Memnon	3.76008	0.0001	7.516			False half solution, Ďurech et al. (2020) derived a unique model from the same data
7783 1994 JD	15.9087	0.01	31.83		✓	False half period
10 704 1981 RQ1	3.75401	0.00005	7.507		✓	False half period. Erasmus et al. (2020) have the correct double period from the same data
18 582 1997 XK9	107.7121	0.01	114	✓	✓	We consider these periods to be the same within their uncertainty intervals
$N_{BS} = 22$						
282 Clorinde	49.3623	0.02	6.42	✓	✓	Confirmed by Ďurech et al. (2020) and Bonamico and van Belle (2021)
518 Halawe	7.15908	0.0003	14.31			False half period
1949 Messina	3.39064	0.0002	3.6491		✓	False period
7937 1990 QA2	3.11685	0.0002	6.23		✓	Probably false half period
10 037 1984 BQ	7.854744	0.00007	6.7482		✓	Probably incorrect P_A

records and original publications to decide which period was the correct one. In 14 cases, we concluded that the ATLAS period was correct; in four cases, the LCDB period was correct; and in one case, the asteroid is tumbling, so there is no single rotation period.

So in 885 cases out of 904, P_A and P_{DB} are the same (within a 5% interval), and we assume that these periods are correct—they are real rotation periods. The number of incorrect LCDB periods in our sample is 14 out of 904, so the probability that for a randomly

TABLE 3 | For asteroids with $N_{BS} \geq 20$, the table lists their rotation period P_A , the standard error σ_{BS} estimated from bootstrap, the uncertainty σ_{max} of the period estimated from the length of the observing interval, and the number N_{BS} of cases when P_A was the same as $P_{BS}^{(i)}$. The probability of P_A being correct is directly related to N_{BS} according to **Table 1**. The complete table with more than 5000 records is available as **Supplementary Material**.

Asteroid	P_A (h)	σ_{BS} (h)	σ_{max} (h)	N_{BS}
13	Egeria	7.04634	0.0008	22
24	Themis	8.37415	0.0006	23
26	Proserpina	13.1054	0.002	21
32	Pomona	9.447690	0.00008	24
33	Polyhymnia	18.60912	0.0008	25
34	Circe	12.174549	0.0001	24
37	Fides	7.3327	0.001	21
42	Isis	13.58272	0.0001	23
48	Doris	11.88992	0.0006	22
49	Pales	20.70814	0.0003	25
:	:	:	:	:
217101	2001 XM29	2.7090	0.0001	23
217298	2004 JY4	38.02	0.07	20
222655	2001 XW186	3.36568	0.0004	21
231865	2000 SY318	3.01651	0.0002	23
250436	2003 WT137	8.05050	0.0009	21
267090	1999 VS198	8.9523	0.003	23
270324	2001 XV96	88.0955	0.08	23
350872	2002 PG43	19.710	0.03	20
373534	2001 TR169	5.06367	0.0006	20
411201	2010 LJ14	114.23302	0.008	23



chosen asteroid P_{DB} is not correct (for $U = 3$) is 1.6%. In other words, we estimated that the probability of a period in the LCDB with $U = 3$ being correct is $p_{DB}^{correct} = 98.4\%$.

We compared ATLAS and LCDB periods also for asteroids with $N_{BS} = 24, 23, 22$ and inspected the discrepant cases (**Table 2**). The results are summarized in **Table 1**. The probability that for a

given asteroid both periods are correct is a product of probabilities $p_A^{correct}$ that P_A is correct and $p_{DB}^{correct}$ that P_{DB} is correct. From the analysis of the group of asteroids with $N_{BS} = 25$, we know that $p_{DB}^{correct} = 98.4\%$, so we can compute $p_A^{correct}$. The table lists these probabilities for $N_{BS} \geq 17$. Probability $p_A^{correct}$ is

> 95% for $N_{BS} \geq 22$, for $N_{BS} = 21$ or 20 it is around 93%, and it drops below 90% for $N_{BS} < 20$.

The analysis above depends on the total number of BS samples, however, not critically. If, for some reason, we had only 22 BS samples in total, then for $N_{BS} = 22$ (according to **Table 1**), $N_A = 3885$, $N_{U3} = 1414$, $N_{same} = 1377$, $p_{same} = 97.4\%$, $N_{DB}^{wrong} = 21$, $p_{DB}^{wrong} = 1.5\%$, and $p_A^{correct} = 98.9\%$. So our new estimate of the probability p_{DB}^{wrong} would be almost the same as before and $p_A^{correct}$ would be somewhere between previous values of probabilities determined for $N_{BS} = 22, 23, 24, 25$.

3.2 Periods From ATLAS Data

In total, the sample of asteroids with $p_{DB}^{correct} > 90\%$ consists of 5126 period determinations (we excluded those listed in **Table 2** as not correct and other 55 asteroids that were affected by large systematic errors in their input photometric data). We consider the probability > 90% high enough to publish these periods; they are provided as **Supplementary Material** to this paper. In **Table 3**, we list a small fraction of the results as an example. The uncertainty σ_{BS} of the rotation period is determined as a standard deviation of values $P_{BS}^{(i)}$ that agree with P_A . In many cases, this error is unrealistically small. Therefore, as a conservative upper limit of the period uncertainty, we define $\sigma_{max} = 0.1 \cdot 0.5P_A^2/\Delta$, where Δ is the length of the time interval covered by the data. This uncertainty of the sidereal rotation period corresponds to a shift of 1/20 in the rotation phase over the interval Δ (Kaasalainen, 2004). If σ_{BS} is significantly (several times) larger than σ_{max} and P_A is close to 24 h, it is a strong indication that the detected period is not the true rotation period of the asteroid but a false alias period related to 1-day sampling of the data. As can be seen in **Figure 3** on a histogram of periods, for asteroids with $\sigma_{BS}/\sigma_{max} > 10$, there is an excess of those with the rotation period close to 24 h. These are mostly false-positive solutions that consistently yield the same rotation period of ~24 h for all BS samples, but it is a bias caused by the observations being carried out at one location. The 1-day pattern in the data is inevitable for all BS samples.

For a part of asteroids with our ATLAS-based period determination, their rotation period was already known, sometimes also with a corresponding shape model. Namely, there are 3526 asteroids for which some period is reported in the LCDB; however, the number of reliable periods with $U = 3$ is only 1616. For 1600 asteroids, we derived their rotation period for the first time.

In **Figure 4**, we show a similar plot as Pál et al. (2020), namely the comparison of distribution of periods from the LCDB, TESS, and our ATLAS results. Although there is an apparent lack of long periods in our results when compared with TESS results of Pál et al. (2020), ATLAS sparse photometry can be used for an efficient determination of rotation periods of the order of hundreds of hours. Recent results of Erasmus et al. (2021) show that ground-based surveys are capable of detection rotation periods even longer than thousand hours. However, for the majority of asteroids in our sample, we were not able to determine their rotation period, so it is not possible to use the derived periods for statistical studies without properly accounting for bias.

4 CONCLUSION

We have derived sidereal rotation periods for more than 5000 asteroids; for more than 1600, it is the first period determination. The reliability of these periods is > 90%, so some periods can be incorrect, but the whole sample is a significant increase in the number of asteroids with a known rotation period. The method of bootstrapping the original data is simple to implement, although computationally demanding. The same approach can also be used to new ATLAS data, ideally combined with other sparse photometry, for example, from Gaia Data Release 3.

DATA AVAILABILITY STATEMENT

The data analyzed in this study is subject to the following licenses/restrictions: ATLAS photometry. Requests to access these datasets should be directed to <https://atlas.fallingstar.com>.

AUTHOR CONTRIBUTIONS

JĎ—ATLAS data processing, bootstrap, interpretation; MV—processing of bootstrapped periodograms, interpretation; RV—technical administration of the Asteroids@home project; NE—ATLAS scientist.

FUNDING

This work has been supported by the grant 20-08218S of the Czech Science Foundation. This work has made use of data from the Asteroid Terrestrial-impact Last Alert System (ATLAS) project. ATLAS is primarily funded to search for near earth asteroids through NASA grants NN12AR55G, 80NSSC18K0284, and 80NSSC18K1575; byproducts of the NEO search include images and catalogs from the survey area. The ATLAS science products have been made possible through the contributions of the University of Hawaii Institute for Astronomy, the Queen's University Belfast, the Space Telescope Science Institute, and the South African Astronomical Observatory (SAAO), and the Millennium Institute of Astrophysics (MAS), Chile.

ACKNOWLEDGMENTS

We greatly appreciate the contribution of tens of thousands of volunteers who joined the Asteroids@home BOINC project and provided their computing resources. This research has made use of IMCCE's Miriade VO tool.

SUPPLEMENTARY MATERIAL

The Supplementary Material for this article can be found online at: <https://www.frontiersin.org/articles/10.3389/fspas.2022.809771/full#supplementary-material>

REFERENCES

- Barucci, M. A., di Martino, M., Dotto, E., Fulchignoni, M., Rotundi, A., and Burchi, R. (1994). Rotational Properties of Small Asteroids: Photoelectric Observations of 16 Asteroids. *Icarus* 109, 267–273. doi:10.1006/icar.1994.1092
- Bennefeld, C., Bass, S., Blair, R., Cunningham, K., Hill, D., McHenry, M., et al. (2009). Asteroid Lightcurve Analysis at Ricky Observatory. *Minor. Planet. Bull.* 36, 147–148.
- Binzel, R. P. (1987). A Photoelectric Survey of 130 Asteroids. *Icarus* 72, 135–208. doi:10.1016/0019-1035(87)90125-4
- Bonamico, R., and van Belle, G. (2021). Determining the Rotational Period of Main-Belt Asteroid 282 Clorinde. *Minor. Planet. Bull.* 48, 210.
- Childers, D., and Church, A. (2007). High-speed Photometric Analysis for Minor Planets 1586 Thiele, 4246 Telemann, (10662) 32-1 T-2, and (49880) 1999 XP 135. *Minor. Planet. Bull.* 34, 124–125.
- Devogèle, M., Tanga, P., Bendjoya, P., Rivet, J. P., Surdej, J., Hanuš, J., et al. (2017). Shape and Spin Determination of Barbarian Asteroids. *A&A* 607, A119. doi:10.1051/0004-6361/201630104
- Đurech, J., Hanuš, J., and Ali-Lagoa, V. (2018). Asteroid Models Reconstructed from the Lowell Photometric Database and WISE Data. *A&A* 617, A57. doi:10.1051/0004-6361/201833437
- Đurech, J., Hanuš, J., Oszkiewicz, D., and Vančo, R. (2016). Asteroid Models from the Lowell Photometric Database. *A&A* 587, A48. doi:10.1051/0004-6361/201527573
- Đurech, J., and Hanuš, J. (2018). Reconstruction of Asteroid Spin States from Gaia DR2 Photometry. *A&A* 620, A91. doi:10.1051/0004-6361/201834007
- Đurech, J., Hanuš, J., and Vančo, R. (2015). Asteroids@home-A BOINC Distributed Computing Project for Asteroid Shape Reconstruction. *Astron. Comput.* 13, 80–84. doi:10.1016/j.ascom.2015.09.004
- Đurech, J., Hanuš, J., and Vančo, R. (2019). Inversion of Asteroid Photometry from Gaia DR2 and the Lowell Observatory Photometric Database. *A&A* 631, A2. doi:10.1051/0004-6361/201936341
- Đurech, J., Kaasalainen, M., Warner, B. D., Fauerbach, M., Marks, S. A., Fauvaud, S., et al. (2009). Asteroid Models from Combined Sparse and Dense Photometric Data. *A&A* 493, 291–297. doi:10.1051/0004-6361/200810393
- Đurech, J., Tonry, J., Erasmus, N., Denneau, L., Heinze, A. N., Flewelling, H., et al. (2020). Asteroid Models Reconstructed from ATLAS Photometry. *A&A* 643, A59. doi:10.1051/0004-6361/202037729
- Erasmus, N., Kramer, D., McNeill, A., Trilling, D. E., Janse van Rensburg, P., van Belle, G. T., et al. (2021). Discovery of Superslow Rotating Asteroids with ATLAS and ZTF photometry. *MNRAS* 506, 3872–3881. doi:10.1093/mnras/stab1888
- Erasmus, N., Navarro-Meza, S., McNeill, A., Trilling, D. E., Sickafoose, A. A., Denneau, L., et al. (2020). Investigating Taxonomic Diversity within Asteroid Families through ATLAS Dual-Band Photometry. *ApJS* 247, 13. doi:10.3847/1538-4365/ab5e88
- Franco, L., and Pilcher, F. (2020). Spin-Shape Model for 50 Virginia. *Minor. Planet. Bull.* 47, 272–274.
- Hanuš, J., Đurech, J., Brož, M., Marciniak, A., Warner, B. D., Pilcher, F., et al. (2013). Asteroids' Physical Models from Combined Dense and Sparse Photometry and Scaling of the YORP Effect by the Observed Obliquity Distribution. *A&A* 551, A67. doi:10.1051/0004-6361/201220701
- Hanuš, J., Đurech, J., Oszkiewicz, D. A., Behrend, R., Carry, B., Delbo, M., et al. (2016). New and Updated Convex Shape Models of Asteroids Based on Optical Data from a Large Collaboration Network. *Astron. Astrophys.* 586, A108. doi:10.1051/0004-6361/201527441
- Hanuš, J., Pejcha, O., Shappee, B. J., Kochanek, C. S., Stanek, K. Z., and Holoiu, T. W. S. (2021). V-band Photometry of Asteroids from ASAS-SN. Finding Asteroids with Slow Spin. *Astron. Astrophys.* 654, A48. doi:10.1051/0004-6361/202140759
- Heinze, A. N., Tonry, J. L., Denneau, L., Flewelling, H., Stalder, B., Rest, A., et al. (2018). A First Catalog of Variable Stars Measured by the Asteroid Terrestrial-Impact Last Alert System (ATLAS). *Aj* 156, 241. doi:10.3847/1538-3881/aae47f
- Hušárik, M. (2018). Shape Model of the Asteroid (2501) Lohja from Long-Term Photometric Observations. *Contrib. Astronomical Observatory Skalnaté Pleso* 48, 319–328.
- Kaasalainen, M., and Đurech, J. (2020). Asteroid Models from Generalised Projections: Essential Facts for Asteroid Modellers and Geometric Inverse Problem Solvers. arXiv e-prints, arXiv:2005.09947.
- Kaasalainen, M., Mottola, S., and Fulchignoni, M. (2002). "Asteroid Models from Disk-Integrated Data," in *Asteroids III*. Editors W. F. Bottke, A. Cellino, P. Paolicchi, and R. P. Binzel (Tucson: University of Arizona Press), 139–150. doi:10.2307/j.ctv1v7zdn4.17
- Kaasalainen, M. (2004). Physical Models of Large Number of Asteroids from Calibrated Photometry Sparse in Time. *A&A* 422, L39–L42. doi:10.1051/0004-6361:20048003
- Kaasalainen, M., Torppa, J., and Muinonen, K. (2001). Optimization Methods for Asteroid Lightcurve Inversion II. The Complete Inverse Problem. *Icarus* 153, 37–51. doi:10.1006/icar.2001.6674
- Marciniak, A., Bartczak, P., Müller, T., Sanabria, J. J., Ali-Lagoa, V., Antonini, P., et al. (2018). Photometric Survey, Modelling, and Scaling of Long-Period and Low-Amplitude Asteroids. *A&A* 610, A7. doi:10.1051/0004-6361/201731479
- Pál, A., Szakáts, R., Kiss, C., Bódi, A., Bognár, Z., Kalup, C., et al. (2020). Solar System Objects Observed with TESS-First Data Release: Bright Main-belt and Trojan Asteroids from the Southern Survey. *ApJS* 247, 26. doi:10.3847/1538-4365/ab64f0
- Pilcher, F., Franco, L., and Pravec, P. (2017). 299 Thora and 496 Gryphia: Two More Very Slowly Rotating Asteroids. *Minor. Planet. Bull.* 44, 270–274.
- Polakis, T. (2020). Photometric Observations of Thirty Minor Planets. *Minor. Planet. Bull.* 47, 177–186.
- Smith, K. W., Smartt, S. J., Young, D. R., Tonry, J. L., Denneau, L., Flewelling, H., et al. (2020). Design and Operation of the ATLAS Transient Science Server. *Pasp* 132, 085002. doi:10.1088/1538-3873/ab936e
- Stephens, R. D. (2011). Asteroids Observed From GMARS and Santana Observatories: 2010 October-December. *Minor Planet Bulletin* 38, 115.
- Stephens, R. D. (2002). Photometry of 769 Tatjana, 818 Kapteyna, 1922 Zulu, and 3687 Dzus. *Minor. Planet. Bull.* 29, 72.
- Stephens, R. D., Pilcher, F., Buchheim, R. K., Benishek, V., and Warner, B. D. (2010). Lightcurve Analysis of 740 Cantabia. *Minor. Planet. Bull.* 37, 17.
- Tonry, J. L., Denneau, L., Flewelling, H., Heinze, A. N., Onken, C. A., Smartt, S. J., et al. (2018a). The ATLAS All-Sky Stellar Reference Catalog. *ApJ* 867, 105. doi:10.3847/1538-4357/aae386
- Tonry, J. L., Denneau, L., Heinze, A. N., Stalder, B., Smith, K. W., Smartt, S. J., et al. (2018b). ATLAS: A High-Cadence All-Sky Survey System. *Pasp* 130, 064505. doi:10.1088/1538-3873/aabadf
- Wang, X., Muinonen, K., Wang, Y., Behrend, R., Goncalves, R., Oey, J., et al. (2015). Photometric Analysis for the Spin and Shape Parameters of the C-type Main-belt Asteroids (171) Ophelia and (360) Carola. *A&A* 581, A55. doi:10.1051/0004-6361/201526523
- Warner, B. D., Pravec, P., Kusnirak, P., Benishek, V., and Ferrero, A. (2017). Preliminary Pole and Shape Models for Three Near-Earth Asteroids. *Minor. Planet. Bull.* 44, 203–212.
- Warner, B. D., Harris, A. W., and Pravec, P. (2009). The Asteroid Lightcurve Database. *Icarus* 202, 134–146. doi:10.1016/j.icarus.2009.02.003
- Waszczak, A., Chang, C.-K., Ofek, E. O., Laher, R., Masci, F., Levitan, D., et al. (2015). Asteroid Light Curves from the Palomar Transient Factory Survey: Rotation Periods and Phase Functions from Sparse Photometry. *Aj* 150, 75. doi:10.1088/0004-6256/150/3/75

Conflict of Interest: The authors declare that the research was conducted in the absence of any commercial or financial relationships that could be construed as a potential conflict of interest.

Publisher's Note: All claims expressed in this article are solely those of the authors and do not necessarily represent those of their affiliated organizations, or those of the publisher, the editors and the reviewers. Any product that may be evaluated in this article, or claim that may be made by its manufacturer, is not guaranteed or endorsed by the publisher.

Copyright © 2022 Đurech, Vávra, Vančo and Erasmus. This is an open-access article distributed under the terms of the Creative Commons Attribution License (CC BY). The use, distribution or reproduction in other forums is permitted, provided the original author(s) and the copyright owner(s) are credited and that the original publication in this journal is cited, in accordance with accepted academic practice. No use, distribution or reproduction is permitted which does not comply with these terms.